

Golden mean renormalization for the almost Mathieu operator and related skew products

Hans Koch¹

Department of Mathematics, The University of Texas at Austin, Austin, TX 78712.

Abstract. Considering $\mathrm{SL}(2, \mathbb{R})$ skew-product maps over circle rotations, we prove that a renormalization transformation associated with the golden mean α_* has a nontrivial periodic orbit of length 3. We also present some numerical results, including evidence that this period 3 describes scaling properties of the Hofstadter butterfly near the top of the spectrum at α_* , and scaling properties of the generalized eigenfunction for this energy.

1. Introduction

We consider a renormalization transformation that arises in the study of the spectrum of Schrödinger operators

$$(H^\alpha u)_n = u_{n+1} + u_{n-1} + V(x_n)u_n, \quad n \in \mathbb{Z}, \quad (1.1)$$

acting on sequences $u \in \ell^2(\mathbb{Z})$. Here, V is a suitable potential, and $x_n = x_0 + n\alpha$ for some given real number α . Potentials for which $n \mapsto V(x_n)$ is quasiperiodic lead to interesting spectra and have attracted considerable attention. The equation $H^\alpha u = Eu$ for an eigenvector or generalized eigenvector of H^α can be written as

$$\begin{bmatrix} u_{n+1} \\ u_n \\ u_{n-1} \end{bmatrix} = A(x_n) \begin{bmatrix} u_n \\ u_{n-1} \end{bmatrix}, \quad A(x) = \begin{bmatrix} E - V(x) & -1 \\ 1 & 0 \end{bmatrix}. \quad (1.2)$$

The motivating example for the work presented here is the almost Mathieu (AM) operator, which corresponds to a potential $V(x) = 2\lambda \cos(2\pi(x + \xi))$. Two reviews can be found in [16,28]. By adding $1/2$ to ξ , if necessary, we may assume that $\lambda \geq 0$. A quantity of interest here is the rotation number

$$\mathrm{rot}(\alpha, E) = \lim_{N \rightarrow \infty} \frac{\Sigma_N(\alpha, E)}{2N}, \quad (1.3)$$

where $\Sigma_N(\alpha, E)$ denotes the number of sign changes of a nontrivial solution $n \mapsto u_n$, as n ranges from 1 to N . For any fixed value of $x_0 + \xi$, the rotation number $\mathrm{rot}(\alpha, E)$ is independent of u and depends continuously on α and E . If α is irrational, then $\mathrm{rot}(\alpha, E)$ is independent of the choice of $x_0 + \xi$ as well, by ergodicity. For proof of these and other properties (mentioned below) of the rotation number, we refer to [6,7,9].

The AM Hamiltonian H^α is a “reduced” form of the Hofstadter Hamiltonian [1,2], which describes Bloch electrons moving on \mathbb{Z}^2 , under the influence of a magnetic flux $2\pi\alpha$ through each unit cell. For $\lambda < 1$ the system is conducting (purely ac spectrum), and for $\lambda > 1$ it is insulating (purely pp spectrum), for almost every value of α and $x_0 + \xi$. For details, including proofs and references, see [22]. The Hofstadter Hamiltonian has an

¹ Email: koch@math.utexas.edu

obvious duality transformation, which corresponds to replacing λ by λ^{-1} and E by $\lambda^{-1}E$. In the self-dual case $\lambda = 1$, the spectrum of H^α is included in the interval $[-4, 4]$, and when plotted as a function of $\alpha \in [0, 1]$, it is known as the Hofstadter butterfly [2]. It has zero Lebesgue measure [14,27] and interesting topological properties [24]. The spectrum itself is purely singular-continuous [20,27], for all irrational α and almost every $x_0 + \xi$.

The Hofstadter butterfly is symmetric with respect to the reflections $\alpha \mapsto 1 - \alpha$ and $E \mapsto -E$. The positive-energy part is shown in Figure 1. The solid regions represent gaps in the spectrum, which are open intervals for fixed α ; and their colors encode the so-called gap index $k \in \mathbb{Z}$. To be more precise, the function $\alpha \mapsto \text{rot}(\alpha, E)$ is constant on the gap with index k , where it satisfies

$$1 - 2 \text{rot}(\alpha, E) \equiv k\alpha \pmod{1}. \quad (1.4)$$

The left hand side of this congruence can also be identified with the integrated density of states [5,7,15,29], which makes (1.4) a purely spectral relation.

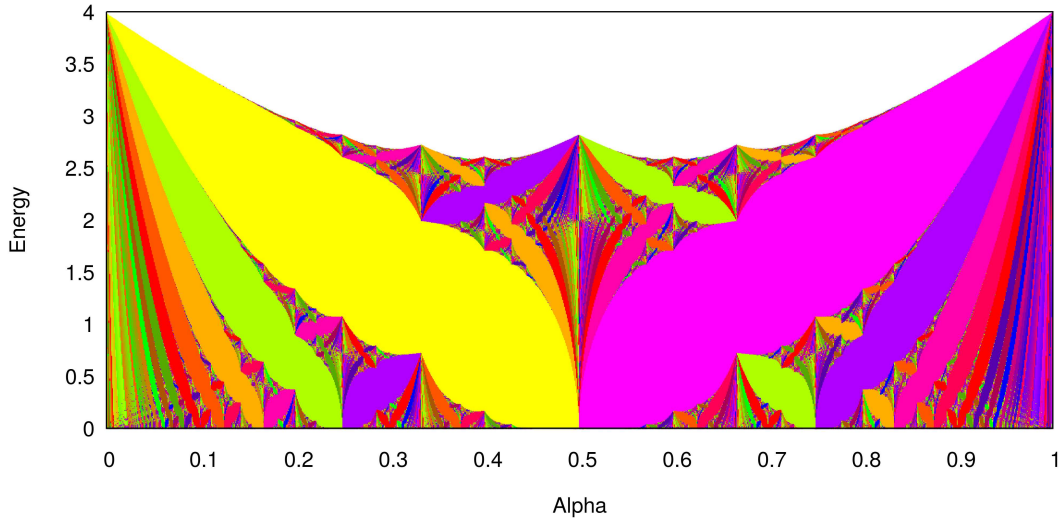


Figure 1. Positive-energy part of the Hofstadter butterfly.

The largest regions are for $k = 1$ (left) and $k = -1$ (right).

A solution u of the equation (1.2) defines an orbit $n \mapsto (x_n, (u_n, u_{n-1}))$ for the following map G :

$$G(x, y) = (x + \alpha, A(x)y), \quad x \in X, \quad y \in \mathbb{R}^2. \quad (1.5)$$

Here, X denotes the real line \mathbb{R} or the circle $\mathbb{T} = \mathbb{R}/\mathbb{Z}$, depending on the situation being considered. A map of this type will be referred to as a skew-product map over a translation of X , or a skew-product (map) for short. Given this connection with dynamics, the Hofstadter butterfly can be viewed as a two-dimensional analogue of the Arnold tongues, which characterize resonances in circle maps. In particular, it exhibits interesting self-similarity properties [21,33]. This strongly suggests the use of renormalization techniques.

Renormalization group (RG) transformations for maps that involve irrational rotations have been studied for a variety of systems, from circle maps and area-preserving maps of

the plane, to skew-products of the type (1.5). Among the many references that could be listed here are [3,4,11,19,27,31]. In essence, these RG transformations lift the Gauss map (defined on $[0, 1]$, mapping $\alpha > 0$ to the fractional part of $1/\alpha$, and zero to zero) to a space of dynamical systems. In order to allow for scaling, they are usually formulated for pairs of commuting maps.

In this paper, we focus on the inverse golden mean $\alpha_* = (\sqrt{5} - 1)/2$, which is a fixed point of the Gauss map. This allows us to consider a single RG transformation \mathfrak{R} . Possible applications include a description of the generalized eigenfunction of the self-dual AM Hamiltonian H^{α_*} for the largest energy value E_* in its spectrum. Another possible application concerns the self-similarity and scaling property of the Hofstadter butterfly, as α approaches α_* and E approaches E_* . This self-similarity is depicted in Figure 2. It shows 4 successive enlargements of the Hofstadter butterfly, zooming in on the point (α_*, E_*) . The largest spectrum-free region in the n -th magnification corresponds to a gap index $k_n = (-1)^n f(n+1)$, where $f(m)$ denotes the m -th Fibonacci number.

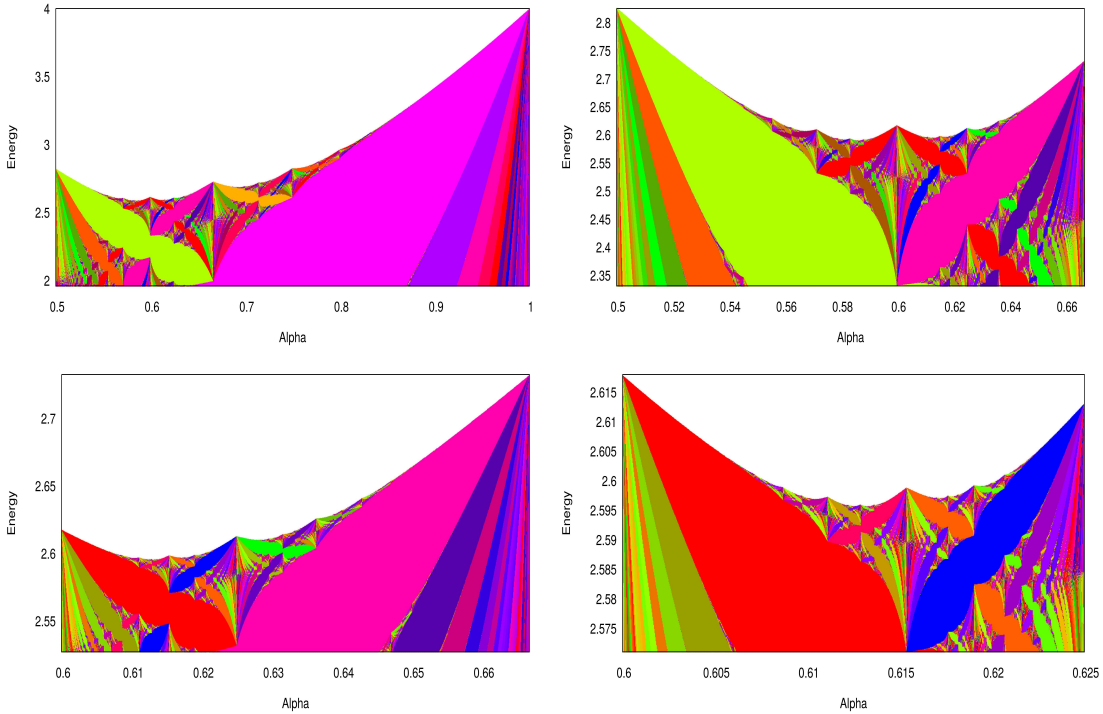


Figure 2. Enlargements of the Hofstadter butterfly for α near α_* .

In order to simplify notation, a skew-product map G of the form (1.5) will be written as (α, A) . Given a second map $F = (\beta, B)$ of the same type, we define the renormalized pair as

$$\mathfrak{R}(P) = \left(\Lambda_1^{-1} G \Lambda_1, \Lambda_1^{-1} F G^{-1} \Lambda_1 \right), \quad P = (F, G). \quad (1.6)$$

Here, Λ_1 is a map on $\mathbb{R} \times \mathbb{R}^2$ of the form $\Lambda_1(x, y) = (\alpha_* x, L(x)y)$, where L depends on the pair P as described below.

The scaling $x \mapsto \alpha_*x$ of the first component is canonical and standard. In order to motivate our choice of L , let us consider the AM map $G = (\alpha, A)$, with A given by (1.2) and $V(x) = 2\lambda \cos(2\pi(x + \xi))$. Since A is periodic with period 1, G commutes with $F = (1, \mathbf{1})$, where $\mathbf{1}$ denotes the 2×2 identity map. This property is preserved under renormalization: if P is a commuting pair, then so is $\mathfrak{R}(P)$. Another noteworthy property of the transformation \mathfrak{R} is that it commutes with the inversion $(F, G) \mapsto (F^{-1}, G^{-1})$ for commuting pairs, modulo a trivial conjugacy. This property has the potential of producing non-uniqueness, in the sense that every RG orbit comes in pairs. There should be no real distinction between such orbits. This brings us to an interesting property of the AM map G : it is reversible, in the sense that

$$G^{-1} = \mathcal{S}_c G \mathcal{S}_c, \quad \mathcal{S}_c(x, y) = (c - x, S y), \quad S = \begin{bmatrix} 0 & 1 \\ 1 & 0 \end{bmatrix}, \quad (1.7)$$

with $c = \alpha - 2\xi$. Notice that \mathcal{S}_c is an involution, meaning that $\mathcal{S}_c^2 = \mathbf{I}$.

One of the lesson learned from the RG analysis of area-preserving maps [19,31] is that reversibility should be preserved under renormalization, if possible. Thus, we choose Λ_1 to commute with \mathcal{S}_c . For simplicity, we consider $c = 0$ and set

$$\Lambda_1(x, y) = (\alpha_*x, S e^{\sigma_1 S} y). \quad (1.8)$$

The constant $\sigma_1 = \sigma_1(P)$ is chosen in such a way that the renormalized pair $\mathfrak{R}(P)$ satisfies a suitable normalization condition (defined later). Unless specified otherwise, we assume now that $\alpha = \alpha_*$ and $\beta = 1$. This pair of translations reproduces under renormalization, in the sense that $\mathfrak{R}(P) = ((1, B_1), (\alpha_*, A_1))$ for two matrix functions A_1 and B_1 .

Our main result is the following.

Theorem 1.1. *The transformation \mathfrak{R}^3 has a fixed point $P_* = (F_*, G_*)$, with $F_* = (1, B_*)$ and $G_* = (\alpha_*, A_*)$ reversible and mutually commuting. The functions B_* and A_* are non-constant, take values in $\text{SL}(2, \mathbb{R})$ for real arguments, and extend analytically to the entire complex plane. The three-step scaling factor (described below) for P_* is given by*

$$e^{\sigma_*} = 1.7000157758867897671921936150581734037633645686725\dots \quad (1.9)$$

To our knowledge, the existence of such a 3-periodic RG orbit has not been described before in the literature. Some numerical and approximate RG computations can be found in [8,17,23,26], to mention just a few.

To be more precise about the scaling factor e^{σ_*} , we note that \mathfrak{R}^3 is given by

$$\mathfrak{R}^3(P) = (\Lambda_3^{-1} G^2 F^{-1} \Lambda_3, \Lambda_3^{-1} F G^{-1} F G^{-2} \Lambda_3). \quad (1.10)$$

Here, Λ_3 is a composition of three scalings (1.8) and thus of the form

$$\Lambda_3(x, y) = (\alpha_*^3 x, S e^{\sigma_3 S} y). \quad (1.11)$$

The scaling parameter $\sigma_3 = \sigma_3(P)$ is determined by a suitable normalization condition for the pair $\mathfrak{R}^3(P)$. For the precise definition we refer to Section 3. The constant σ_* that appears in (1.9) is the value of $\sigma_3(P_*)$. It is independent of the choice of normalization.

Our proof of Theorem 1.1 relies on estimates that have been carried out with the aid of a computer; see Sections 3, 4, and 6. As a by-product we obtain highly accurate estimates on various relevant quantities, including the function A_* and B_* . Some bounds are given in Lemma 3.1.

The same techniques can be used to prove the existence of a fixed point for \mathfrak{R}^6 that is associated with energy $E = 0$. This and related result will be published elsewhere [37]. In addition, recent numerical findings [36] suggest that \mathfrak{R} has an infinite number of periodic orbits, associated with certain rational rotation numbers, and describing scaling properties of the Hofstadter butterfly for $\alpha = \alpha_*$. The most prominent accumulation phenomenon occurs at the point $(\alpha, E) = (0, 0)$. A scaling conjecture and some related work can be found in [10,12,14].

Following an idea that was used in [19,31], we solve the fixed point equation for \mathfrak{R}^3 by first solving the fixed point equation for the following “palindromic” modification:

$$\mathfrak{R}_3(P) = (\Lambda_3^{-1}GF^{-1}G\Lambda_3, \Lambda_3^{-1}G^{-1}FG^{-1}FG^{-1}\Lambda_3). \quad (1.12)$$

Clearly, $\mathfrak{R}_3(P)$ agrees with $\mathfrak{R}^3(P)$, if P is a commuting pair. The advantage of the transformation \mathfrak{R}_3 is that it preserves reversibility, even for pairs that do not commute. The condition $FG = GF$ is very inconvenient to work with, so we drop it while solving the fixed point equation for \mathfrak{R}_3 . Once a solution P_* is found, it is not too hard to show that F_* and G_* have to commute.

At this time, our evidence that the behavior of \mathfrak{R} near P_* describes properties of the spectrum and generalized eigenfunctions for the self-dual AM model is purely numerical. Our numerical results are described in Section 2. In particular, they indicate that the following applies to the self-dual AM model with $\alpha = \alpha_*$ and $E = E_*$.

Theorem 1.2. *Let $G = (\alpha_*, A)$ be a continuous skew-product map on $\mathbb{T} \times \mathbb{R}^2$, such that $P = ((1, 1), G)$ is infinitely renormalizable. To be more precise, write $P_n = \mathfrak{R}^n(P)$ as $P_n = ((1, B_n), (\alpha_*, A_n))$. Assume that the sequence $n \mapsto A_n(x)$ is bounded for some x , and that $\sigma_3(P_{3k}) > 0$ for large k . Then G has a nontrivial orbit that returns infinitely often to some fixed bounded set. In particular, if A is of the form (1.2), then E belongs to the spectrum of the corresponding Schrödinger operator (1.1).*

A proof of this theorem is given in Section 5. We note that the asymptotic condition $\sigma_3(P_{3k}) > 0$ holds e.g. if $B_{3k} \rightarrow B_*$ and $A_{3k} \rightarrow A_*$, uniformly on the interval $(-2, 2)$.

In summary, we describe here a new approach to the asymptotic analysis of skew-product maps of the type (1.5). Our use of RG methods is motivated by the well-known observation of self-similarity and scaling in the Hofstadter spectrum. Renormalization, as developed in the theory of critical phenomena, focuses on a specific point in the phase diagram. For simplicity, and as a first step, we have chosen the point (α_*, E_*) in the Hofstadter spectrum. Many other scaling points should be accessible by the same methods. Besides determining an appropriate RG transformation \mathfrak{R} , the first step in a renormalization analysis of this type is to find a relevant invariant set for \mathfrak{R} , preferably a periodic point. This part is the intended goal of the present paper, with the choice of \mathfrak{R} and Theorem 1.1 being the main results. The relevance of \mathfrak{R} to the spectral problem is illustrated

by Theorem 1.2. Some additional, but purely numerical results are described in the next section. Numerically, there is no doubt that our 3-periodic orbit P_* of \mathfrak{R} , and the expanding eigenvalues of the derivative $D\mathfrak{R}^3(P_*)$, describe the scaling properties of the Hofstadter spectrum near the point (α_*, E_*) . A rigorous proof of this claim looks possible but would go far beyond the scope of the present paper.

2. Some numerical results and observations

Figure 3 shows the matrix A_* described in Theorem 1.1 as a function of x . To be more specific, let us first change basis and write $A_{\text{new}} = MA_{\text{old}}M$ and $S_{\text{new}} = MS_{\text{old}}M$, with $M = M^{-1}$ as defined below. The matrices $A = A_{\text{new}}$ and $S = S_{\text{new}}$ are of the form

$$A = \begin{bmatrix} t+s & u \\ v & t-s \end{bmatrix}, \quad S = \begin{bmatrix} 1 & 0 \\ 0 & -1 \end{bmatrix}, \quad M = \frac{1}{\sqrt{2}} \begin{bmatrix} 1 & 1 \\ 1 & -1 \end{bmatrix}. \quad (2.1)$$

From now on, reversibility is defined with respect to this new matrix S . Notice that the matrix part of the scaling Λ_3 is diagonal in these new coordinates, with eigenvalue entries e^{σ_3} and $-e^{-\sigma_3}$.

In this representation, the Schrödinger matrix (1.2) corresponds to $t = (E - V)/2$, $u = t + 1$, $v = t - 1$, and $s = 0$. If A is the second component of a map $G = (\alpha, A)$, then we usually work with the translated matrix $A_0(x) = A(x - \frac{\alpha}{2})$, so that G is reversible if and only if the components t_0, u_0, v_0 of A_0 are even, and s_0 is odd. These components for the matrix A_* are shown in Figure 3.

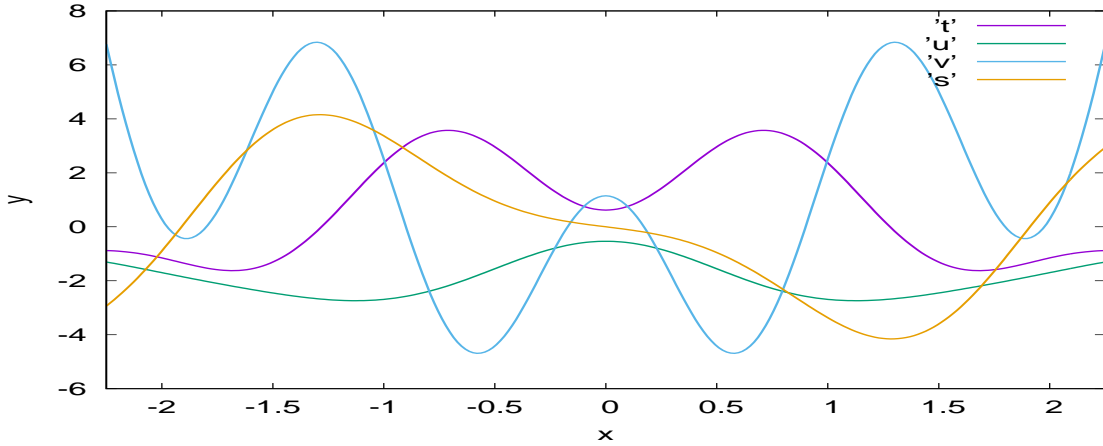


Figure 3. Components of the matrix A_0 for the skew-product map G_* .

Our proof of Theorem 1.1 involves the use of an approximate fixed point \bar{P} for \mathfrak{R}_3 . A first rough approximation was found by computing iterates $P_n = \mathfrak{R}^n(P)$ for the self-dual AM model with $\alpha = \alpha_*$, while adjusting the energy (via bisection) to get $k \mapsto P_{3k}$ to converge numerically. Better approximations are then obtained easily by using the contraction \mathfrak{M} described in Section 3.

The approximate eigenfunction u mentioned in Theorem 1.2 is shown in Figure 4, for the self-dual AM map with $\alpha = \alpha_*$, energy $E_* = 2.5975151853767716484693511092199\dots$,

and starting point $x_0 + \xi = \alpha/2$. The vector $y_n = (u_{n-1}, u_n)$ for $n = 0$ is the expanding eigenvector $\begin{bmatrix} 1 \\ 0 \end{bmatrix}$ of the scaling Λ_3 . The vector y_n at the m -th Fibonacci number $n = f(m)$ is again asymptotically (for large m) parallel to $\begin{bmatrix} 1 \\ 0 \end{bmatrix}$, with length of order 1.

Figure 4 consists essentially of sharp peaks, even in the “solid” looking regions. The peaks that are higher than all preceding ones are at $n = 1, 6, 27, 116, 493, 2090, 8855, 37512, 158905, 673134, 2851443, \dots$. These values $n(1), n(2), \dots$ fit the formula

$$n(m) = \frac{1}{2}[f(3m+1) - 1]. \quad (2.2)$$

The RG period 3 is clearly visible in these data. Notice that $n(m) \sim \alpha_*^{-3m}$, and the corresponding peaks in Figure 4 grow like $e^{2m\sigma_*}$. The sequence (2.2) appears in other contexts as well and is listed as A049651 in the On-Line Encyclopedia of Integer Sequences. References and links can be found at [35].

Another property of the orbit u depicted in Figure 4 is that $u_n \geq 0$ for all n . This indicates that the AM map G for $E = E_*$ has a zero rotation number. For values of E below E_* , we find positive rotation numbers.

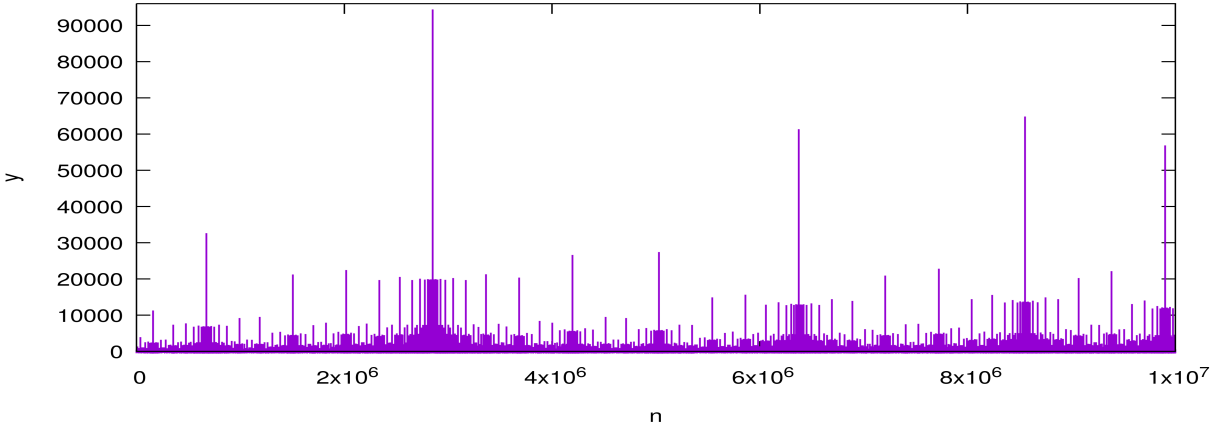


Figure 4. Generalized eigenfunction for the self-dual AM Hamiltonian with $\alpha = \alpha_*$ and $E = E_*$.

Our proof of Theorem 1.1 also involves the use of a modest-size matrix approximation for the derivative $D\mathfrak{R}_3(P_*)$. By increasing the dimension to get a more accurate approximation, the eigenvalues of modulus larger than 1/10 are found to be

$$\begin{aligned} \mu_1 &= 30.79005494022096246\dots, & \mu_{3,4} &= \pm 0.68224911725088276\dots, \\ \mu_2 &= 4.23606797749978969\dots, & \mu_5 &= -0.13757909772243458\dots. \end{aligned} \quad (2.3)$$

The largest eigenvalue, μ_1 , is almost certainly related to the (three generation) scaling of the Hofstadter butterfly in the energy direction. The scaling seen in Figures 1 and 2, averaged over 4 generations, agrees with $\mu_1^{1/3}$ at the accuracy available. The scaling in the α -direction over 3 generation is trivially $-\alpha_*^{-6}$. But our current RG analysis is for the fixed value $\alpha = \alpha_*$, so there is no room for an eigenvector of $D\mathfrak{R}_3(P_*)$ in the direction of a change of α .

Concerning the eigenvalue μ_2 , we conjecture that its value is equal to α_*^{-3} . But despite its “trivial” value, it is not associated with a coordinate change or a non-commuting direction. We believe that μ_2 is related to variations in the strength of the x -dependence. In the AM model, such a change characterizes the transition between the conducting phase $\lambda < 1$ and the insulating phase $\lambda > 1$. A formal argument supporting our conjecture is given in Section 6 and [36].

As in other renormalization schemes in dynamical systems, many of the observed eigenvalues are associated with variations arising from coordinate changes. The largest here seems to be $\mu_3 = -e^{2\sigma_*} \alpha_*^3$. Other trivial eigenvalues of $D\mathfrak{R}_3(P_*)$ arise from variations in the direction of non-commuting pairs. The largest such eigenvalue here is -1 , which we omitted from the list (2.3). These eigenvalues can be determined explicitly, as will be described in Section 6.

More interesting observations are the following. Many trivial eigenvalues are paired with an eigenvalue of opposite sign, such as $\mu_4 = -\mu_3$. We have no explanation for why these eigenvalues should occur. What is particularly intriguing is that even the “relevant” eigenvalue μ_1 appears to be algebraic and related to α_* . As was observed in [36], the eigenvalues μ_1 and μ_5 seem to be the real roots of the quartic equation $z^4 - 30z^3 - 24z^2 - 10z - 1 = 0$. Furthermore, the scaling exponent σ_* agrees to the (high) accuracy available with the value $1/2 \cosh^{-1}(\alpha_*^{-1})$.

It seems likely that the (apparent) algebraic nature of these eigenvalues reflects some algebraic properties of the self-dual Hofstadter Hamiltonian. This Hamiltonian has definitely some interesting symmetries, best known for rational α , and the generalized eigenfunctions for $E = 0$ can be found explicitly in this case [13,18]. But none of these known properties seems to shed any light on the above-mentioned observations.

3. The fixed point problem

In this section we reformulate the equation $\mathfrak{R}_3(P) = P$ as a fixed point problem for a contraction, acting on a suitable space of pairs.

3.1. Normalization

Since the transformation \mathfrak{R}_3 involves the composition and inverses of skew-product maps, let us first describe these two operations. As mentioned in the last section, the matrix part A of a map $G = (\alpha, A)$ is being represented as $A = A_0\left(\frac{\alpha}{2} + .\right)$. Then G is reversible if and only if $A_0^{-1}(x) = SA_0(-x)S$ for all x . The composition of two skew-products is given by

$$(\beta, B)(\alpha, A) = (\alpha + \beta, C), \quad C_0 = B_0\left(\frac{\alpha}{2} + .\right)A_0\left(-\frac{\beta}{2} + .\right). \quad (3.1)$$

In particular, (β, B) is the inverse of (α, A) if and only if $\beta = -\alpha$ and $B_0 = A_0^{-1}$.

Consider now a conjugacy $H \mapsto \Lambda_3^{-1}H\Lambda_3$. In the expression (1.12) for $\mathfrak{R}_3(P)$, such a conjugacy is being applied to $GF^{-1}G$ and $G^{-1}FG^{-1}FG^{-1}$. Consider first $H = GF^{-1}G$, which is of the form $H = (\alpha_*^3, C)$. The matrix part of $\Lambda_3^{-1}H\Lambda_3$ is given by

$$e^{-\sigma_3 S} SCSe^{\sigma_3 S} = \begin{bmatrix} t+s & -e^{-2\sigma_3} u \\ -e^{2\sigma_3} v & t-s \end{bmatrix}, \quad \text{if } C = \begin{bmatrix} t+s & u \\ v & t-s \end{bmatrix}. \quad (3.2)$$

Our normalization condition that determines σ_3 is that $e^{-2\sigma_3}u_0(0)$ and $e^{2\sigma_3}v_0(0)$ have the same absolute value. Clearly, other normalization conditions would work equally well. The same value of σ_3 is used to scale $H = G^{-1}FG^{-1}FG^{-1}$. In other words, only the first component of the pair $\mathfrak{R}_3(F, G)$ is being “re-normalized”. But of course, this affects both components when \mathfrak{R}_3 is being iterated.

3.2. An extension

Given the constructive nature of our analysis, an important question is how to deal with a constraint like $\det(A) = 1$. Typical $\text{SL}(2, \mathbb{R})$ methods, including an Iwasawa-type decomposition for real matrices, involve quantities that have singularities in the complex plane. The resulting bounds were not sufficient for our purpose. For the problem considered here, it is better to consider $\text{PSL}(2, \mathbb{C})$, via Möbius transformations

$$\mathbf{a}z = \frac{az + u}{vz + d}, \quad A = \begin{bmatrix} a & u \\ v & d \end{bmatrix}. \quad (3.3)$$

In particular, our involution is represented by

$$\mathbf{s}z = -z, \quad S = \begin{bmatrix} 1 & 0 \\ 0 & -1 \end{bmatrix}. \quad (3.4)$$

Notice that the transformation \mathbf{a} is well-defined as long as $ad - uv \neq 0$. Our maps $G = (\alpha, A)$ involve matrices $A \in \text{SL}(2, \mathbb{R})$, so the corresponding Möbius transformations \mathbf{a} map the upper half of the extended complex plane $\mathbb{C} \cup \{\infty\}$ into itself. As long as $ad - uv \neq 0$, we have

$$\mathbf{a}^{-1}z = \frac{dz - u}{-vz + a}, \quad \mathbf{s}\mathbf{a}\mathbf{s}z = \frac{az - u}{-vz + d}. \quad (3.5)$$

Consider temporarily $G = (\alpha, \mathbf{a})$ instead of $G = (\alpha, A)$. We say that G is reversible if $\mathcal{S}_0G\mathcal{S}_0 = G^{-1}$, where $\mathcal{S}_0(x, z) = (-x, \mathbf{s}z)$. For the translated quantities described after (2.1) and at the beginning of this section, reversibility means that

$$\mathbf{a}_0(x)^{-1} = \mathbf{s}\mathbf{a}_0(-x)\mathbf{s}, \quad \frac{d_0(x)z - u_0(x)}{-v_0(x)z + a_0(x)} = \frac{a_0(-x)z - u_0(-x)}{-v_0(-x)z + d_0(-x)}. \quad (3.6)$$

In other words, the functions $t_0 = (a_0 + b_0)/2$, u_0 , v_0 are even, and $s_0 = (a_0 - b_0)/2$ is odd. Notice that this does not require that A_0 has determinant 1. And the same applies to the expression $\begin{bmatrix} d & -b \\ -c & a \end{bmatrix}$ for the matrix representing the inverse \mathbf{a}^{-1} .

So for all practical purposes, the constraint $\det(A) = 1$ has been eliminated, albeit at the cost of having more degrees of freedom than necessary.

Motivated by the above, we extend our RG transformation \mathfrak{R}_3 to pairs of maps $P = (F, G)$ that need not be area-preserving. (We call (α, A) area-preserving if A has determinant 1.) Still, it is preferable for the fixed point of \mathfrak{R}_3 to be area-preserving. This can be done e.g. by composing \mathfrak{R}_3 with the normalization map

$$\mathfrak{N}((\alpha, A)) = (\alpha, \mathcal{N}(A)), \quad \mathcal{N}(A) = [\det(A)]^{-1/2}A. \quad (3.7)$$

If the determinant of A is close to 1, then $[\det(A)]^{-1/2}$ is well-defined, and $\mathcal{N}(A)$ has determinant 1. Notice also that, if (α, A) is reversible, then $\det(A_0)$ is an even function, so $(\alpha, \mathcal{N}(A))$ is still reversible. The derivative of \mathcal{N} at A is given by

$$D\mathcal{N}(A)\dot{A} = \det(A)^{-1/2}\dot{A} - \tfrac{1}{2}\det(A)^{-3/2}[ad + d\dot{a} - uv - v\dot{u}]A. \quad (3.8)$$

Our extension of \mathfrak{R}_3 is now defined as

$$\mathfrak{F} = \mathfrak{N} \circ \mathfrak{R}_3, \quad \mathfrak{N}((F, G)) = (\mathfrak{N}(F), \mathfrak{N}(G)). \quad (3.9)$$

We consider this map \mathfrak{F} in a neighborhood of an approximate fixed point \bar{P} . In what follows, the domain of \mathfrak{R}_3 is restricted to pairs $P = (F, G)$ whose components $F = (\beta, B)$ and $G = (\alpha, A)$ are reversible, with $\beta = 1$ and $\alpha = \alpha_*$. The maps F and G need not be area-preserving. But by construction, $\mathfrak{F}(P)$ is a pair of reversible area-preserving maps.

3.3. The contraction

As is common in many computer-assisted proofs, we convert the fixed point problem for the given map \mathfrak{F} to a fixed point problem for a quasi-Newton map \mathfrak{M} associated with \mathfrak{F} . To be more specific, let $I - M$ be an approximate inverse of $I - D\mathfrak{F}(\bar{P})$. Then we define

$$\mathfrak{M}(p) = \mathfrak{F}(\bar{P} + (I - M)p) - \bar{P} + Mp. \quad (3.10)$$

Here, the sum of map-pairs is defined component-wise, and $(\alpha, A_1) + (\alpha, A_2)$ is defined as $(\alpha, A_1 + A_2)$. If \bar{P} is close to being a fixed point of \mathfrak{F} , and if M is chosen properly, we can expect \mathfrak{M} to be a contraction in some neighborhood of \bar{P} . Notice that, if p is a fixed point of \mathfrak{M} , then $P = \bar{P} + (I - M)p$ is a fixed point of \mathfrak{F} .

Now we need to define some function spaces. Given $\rho > 0$, denote by \mathcal{A}_ρ the space of all real analytic functions f on $(-\rho, \rho)$ that have a finite norm

$$\|f\|_\rho = \sum_{n=0}^{\infty} |f_n|\rho^n, \quad f(x) = \sum_{n=0}^{\infty} f_n x^n. \quad (3.11)$$

Of course, every $f \in \mathcal{A}_\rho$ extends to an analytic function on the complex disk $|x| < \rho$. Furthermore, \mathcal{A}_ρ is a Banach algebra under the pointwise product of functions.

The space of matrix functions A_0 whose components t_0, u_0, v_0 , and s_0 belong to \mathcal{A}_ρ will be denoted by \mathcal{A}_ρ^4 . The norm of $A_0 \in \mathcal{A}_\rho^4$ is defined as $\|A_0\|_\rho = \|t_0\|_\rho + \|u_0\|_\rho + \|v_0\|_\rho + \|s_0\|_\rho$. To define a space for pairs of such functions, we first fix a pair $\rho = (\rho_F, \rho_G)$ of positive real numbers. Then we define \mathcal{B}_ρ to be the vector space of all pairs $p = (B_0, A_0)$ in $\mathcal{A}_{\rho_F}^4 \times \mathcal{A}_{\rho_G}^4$, equipped with the norm $\|p\|_\rho = \|B_0\|_{\rho_F} + \|A_0\|_{\rho_G}$. The subspace of reversible pairs is denoted by \mathcal{B}_ρ^r .

Due to the above-mentioned restrictions on the domain of \mathfrak{F} , any skew-product $H = (\gamma, C)$ that appears at some stage in the computation of \mathfrak{F} or \mathfrak{M} has a pre-determined first component γ . Thus, in order to simplify notation related to domains and function spaces, let us now identify such a map H with its translated matrix component $C_0 = C(\cdot - \frac{\gamma}{2})$.

In order for \mathfrak{R} to be defined as a map on \mathcal{B}_ρ , it is necessary and sufficient that

$$\frac{1}{2}\alpha^{-2} \leq \rho_G, \quad \frac{1}{2}\alpha + \alpha\rho_G \leq \rho_F \leq \alpha^{-1}\rho_G. \quad (\text{for } \mathfrak{R}) \quad (3.12)$$

These inequalities are easily satisfied e.g. with $2 = \rho_G \leq \rho_F \leq 3$. But it should be noted that, if P belongs to \mathcal{B}_ρ with ρ satisfying (3.12), then the components of $\mathfrak{R}(P)$ are defined on significantly larger domains. Those larger domains are not disks; however, they improve the domain of iterates of \mathfrak{R} . If we restrict to $\rho_G \leq \rho_F$, then the analogue of the condition (3.12) for the transformation \mathfrak{R}_3 is

$$\frac{1}{2} \leq \rho_G \leq \rho_F \leq \alpha^{-3}\rho_G - \frac{1}{2}\alpha^{-1}. \quad (\text{for } \mathfrak{R}_3) \quad (3.13)$$

This condition is significantly weaker than (3.12).

Lemma 3.1. *Let $\rho = (3, 2)$. Then there exist a pair \bar{P} in \mathcal{B}_ρ^r , a bounded linear operator M on \mathcal{B}_ρ^r , and positive constants ε, K, δ satisfying $\varepsilon + K\delta < \delta$, such that the transformation \mathfrak{M} defined by (3.10) is analytic in B_δ and satisfies*

$$\|\mathfrak{M}(0)\|_\rho \leq \varepsilon, \quad \|D\mathfrak{M}(p)\|_\rho \leq K, \quad p \in B_\delta, \quad (3.14)$$

where B_δ denotes the open ball of radius δ in \mathcal{B}_ρ^r , centered at the origin. Furthermore, for every pair $p \in B_\delta$, the matrix components of $P = \bar{P} + (I - M)p$ are non-constant, $e^{\sigma_3(P)}$ satisfies the bound defined by the right hand side of (1.9), and $\|P - \bar{P}\|_\rho < 10^{-280}$.

Our proof of Lemma 3.1 is computer-assisted and will be described in Section 7. We note that much higher precisions than the one described in this lemma can be achieved quite easily.

4. Proof of Theorem 1.1

Assume that Lemma 3.1 holds. By the contraction mapping principle, the given bounds imply that \mathfrak{M} has a unique fixed point p_* in B_δ . The corresponding function $P_* = \bar{P} + (I - M)p_*$ is a fixed point of \mathfrak{F} , and the last statement in Lemma 3.1 applies to $p = p_*$.

The matrix component B_* of F_* is analytic on the complex disk $|x - \frac{1}{2}| < \rho_F$ of radius $\rho_F = 3$, and the matrix component A_* of G_* is analytic on the complex disk $|x - \frac{\alpha_*}{2}| < \rho_G$ of radius $\rho_G = 2$. A trivial computation shows that the domain radii increase under iteration of \mathfrak{R}_3 by a factor larger than 1. (The factor tends to α_*^{-3} as the number of iterations increases.) This shows that B_* and A_* extend to entire analytic functions.

What remains to be proved is that the maps F_* and G_* commute. To this end, consider the commutator $\Theta = FG(GF)^{-1}$ for a general pair $P = (F, G)$. The commutator for the renormalized pair $\tilde{P} = \mathfrak{R}_3(P)$ is easily found to be

$$\tilde{\Theta} = (G\Lambda)^{-1}\Theta^{-1}(G\Lambda). \quad (4.1)$$

If we write $\Theta = (0, C)$, then $\tilde{\Theta} = (0, \tilde{C})$, with

$$\tilde{C}(x) = e^{-\sigma_3 S} SA(\alpha^3 x)^{-1} C(\alpha^3 x + \alpha)^{-1} A(\alpha^3 x) S e^{\sigma_3 S}. \quad (4.2)$$

Consider a change of variables $x = \frac{1}{2\alpha} + z$. Define $C_1(z) = C(x)$ and $\tilde{C}_1(z) = \tilde{C}(x)$. Then the equation (4.2) becomes

$$\tilde{C}_1(z) = A_1(z)^{-1} C_1(\alpha_*^3 z)^{-1} A_1(z), \quad A_1(z) = A\left(\frac{1}{2}\alpha_*^2 + \alpha_*^3 z\right) S e^{\sigma_* S}. \quad (4.3)$$

Let now $P = P_*$, so that $\tilde{C}_1 = C_1$. We need the identity (4.3) in some (arbitrary small) complex open neighborhood of the origin. It is straightforward to check that all these matrix functions are being evaluated only at points in their domain.

Assume now that the following holds for our fixed point P_* .

Proposition 4.1. *The matrix $A_1(0) = A_0\left(\frac{1}{2}\right) S e^{\sigma_* S}$ has no real or imaginary eigenvalues, and the matrix $C_1(0)$ does not have an eigenvalue -1 .*

Applying (4.3) twice, we also have $C_1(0) = A_2(0)^{-2} C_1(0) A_1(0)^2$. In other words, $C_1(0)$ commutes with $A_1(0)^2$. Consider now a basis in \mathbb{C}^2 where $A_1(0)$ is diagonal. By Proposition 4.1, such a basis exists. Then $A_2(0)$ is diagonal as well, and its eigenvalues are non-real by Proposition 4.1. So the matrix $C_1(0)$ has to be diagonal as well; and in particular, it commutes with $A_1(0)$. Now (4.3) implies that $C_1(0)$ is its own inverse. And $C_1(0)$ has no eigenvalue -1 by Proposition 4.1. So $C_1(0)$ must be the identity matrix.

Assume for contradiction that $C_1 \neq \mathbf{1}$. Then $C_1(z) = \mathbf{1} + z^n [\mathcal{C}_n + \mathcal{O}(1)]$ near the origin, for some nonzero matrix \mathcal{C}_n and some positive integer n . Substituting this expression into (4.3) yields $\mathcal{C}_n = \alpha_*^{3n} A_1(0)^{-1} \mathcal{C}_n A_1(0)$. But this is impossible, with $A_1(0)$ being diagonal and having eigenvalues of modulus 1. So $C_1 = \mathbf{1}$ and thus $\Theta = (0, \mathbf{1})$, implying that F_* and G_* commute.

This concludes the proof of Theorem 1.1, conditioned on the validity of Lemma 3.1 and Proposition 4.1.

5. Recurrent orbits

The main goal here is to give a proof of Theorem 1.2. Let $P = (F, G)$ be a commuting pair of skew-products $F = (1, B)$ and $G = (\alpha_*, A)$, where A and B are functions with values in $\text{SL}(2, \mathbb{R})$. Assume that the renormalized maps

$$F_n = (1, B_n), \quad G_n = (\alpha_*, A_n), \quad (F_n, G_n) = P_n \stackrel{\text{def}}{=} \mathfrak{R}^n(P), \quad (5.1)$$

are all well-defined. This involves a condition on the (real) domains of A and B . It suffices e.g. that F be defined on $I_F = (-\rho_F, \rho_F)$ and G on $I_G = (-\rho_G, \rho_G)$, with ρ_F and ρ_G satisfying (3.12). But in order to avoid domain issues when re-arranging factors, assume that F and G are skew-products on $\mathbb{T} \times \mathbb{R}^2$.

Let $n \mapsto p_n$ be the Fibonacci sequence, defined recursively via $p_0 = 0$, $p_1 = 1$, and $p_n = p_{n-1} + p_{n-2}$ for $n \geq 2$. Let $q_n = p_{n+1}$. Given that F and G commute, we have

$$\begin{aligned} F_n &= \Lambda_n^{-1} F^{p_{n-1}} G^{-q_{n-1}} \Lambda_n, & G_n &= \Lambda_n^{-1} F^{-p_n} G^{q_n} \Lambda_n, & (n \text{ even}), \\ F_n &= \Lambda_n^{-1} F^{-p_{n-1}} G^{q_{n-1}} \Lambda_n, & G_n &= \Lambda_n^{-1} F^{p_n} G^{-q_n} \Lambda_n, & (n \text{ odd}), \end{aligned} \quad (5.2)$$

with Λ_n being a scaling of the form

$$\Lambda_n(x, y) = (\alpha_*^n, S^n e^{\sigma_n S}). \quad (5.3)$$

Here, σ_n is a sum of scaling exponents. More specifically, if n is a multiple of 3, say $n = 3k$, then σ_n is the sum of all exponents $\sigma_3(P_{3m})$ with $m < k$. If n is even, then (5.2) yields

$$F^{-p_n} G^{q_n}(\alpha_*^n x, y) = (\alpha_*^n (x + \alpha_*), e^{\sigma_n S} A_n(x) e^{-\sigma_n S} y). \quad (5.4)$$

A similar identity is obtained if n is odd. But in order to prove Theorem 1.2, it suffices to consider even n . Let $y = \begin{bmatrix} 1 \\ 0 \end{bmatrix}$, so that $Sy = y$. Then the second component in (5.4) is given by

$$y_n \stackrel{\text{def}}{=} e^{\sigma_n S} A_n(x) e^{-\sigma_n S} y = e^{\sigma_n(S-\mathbf{1})} A_n(x) y. \quad (5.5)$$

Assume now that the sequence $n \mapsto A_n(x)$ is bounded for some fixed value of x in the domain of the functions A_n . Assume furthermore that σ_n is positive for sufficiently large n . This holds e.g. if $B_{6k} \rightarrow B_*$ and $A_{6k} \rightarrow A_*$, uniformly on I_F and I_G , respectively, since σ_* is positive by (1.9). Given that $S - \mathbf{1} \leq 0$, we see from (5.5) that the sequence $n \mapsto y_n$ is bounded.

Assume now that $F = (1, \mathbf{1})$. In this case, $G^{q_n}(x, y) = (\alpha_*^n (x + \alpha_*), y_n)$. So the above implies that G has an orbit that returns infinitely often to a fixed bounded set in $\mathbb{T} \times \mathbb{R}^2$, as was claimed in Theorem 1.2. The assertion concerning Schrödinger operators is an immediate consequence of this recurrence.

6. Some trivial eigenvalues

A well-known source of trivial eigenvalues in the renormalization of dynamical systems are coordinate changes. For pairs of maps, another source can be the scaling behavior of the commutator; see e.g. [34]. For the skew-product maps considered here, there may be another quantity whose scaling produces a trivial value α^{-3} for the eigenvalue μ_2 . A possibility will be mentioned at the end of this section. Since the spectrum of $D\mathfrak{R}_3(P_*)$ is not the main topic of this paper, we shall keep this section short and thus mostly formal.

6.1. Coordinate changes

For simplicity, let us replace the scaling Λ_3 in the definition (1.12) of \mathfrak{R}_3 by the scaling Λ_* for the fixed point P_* . This produces some extra eigenvalues for $D\mathfrak{R}_3(P_*)$, but these can easily be identified. Under a change of coordinates H_ε we have

$$\mathfrak{R}_3(H_\varepsilon^{-1} P_* H_\varepsilon) = (\Lambda_*^{-1} H_\varepsilon \Lambda_*)^{-1} P_* (\Lambda_*^{-1} H_\varepsilon \Lambda_*). \quad (6.1)$$

Setting $H_\varepsilon = \mathbf{I} + \varepsilon \dot{H} + \mathcal{O}(\varepsilon^2)$ and differentiating with respect to ε yields

$$D\mathfrak{R}_3(P_*) P_{\dot{H}} = P_{\Lambda_*^{-1} \dot{H} \Lambda_*}, \quad P_{\dot{H}} \stackrel{\text{def}}{=} \frac{d}{d\varepsilon} H_\varepsilon^{-1} P_* H_\varepsilon \Big|_{\varepsilon=0}, \quad (6.2)$$

with the map $\dot{H} \mapsto P_{\dot{H}}$ being linear. In particular, if $\Lambda_*^{-1}\dot{H}\Lambda_* = \kappa\dot{H}$, then $P_{\dot{H}}$ is an eigenvector of $D\mathfrak{R}_3(P_*)$ with eigenvalue κ .

Since our analysis is for fixed circle rotations, let us consider just $\dot{H} = (0, \dot{C})$. Near the origin we have $\dot{C}(x) = x^n[\mathcal{C}_n + \mathcal{O}(1)]$ for some nonnegative integer n . Then the eigen-equation $\Lambda_*^{-1}\dot{H}\Lambda_* = \kappa_n\dot{H}$ yields

$$\alpha_*^{3n}\mathcal{S}^{-1}\mathcal{C}_n\mathcal{S} = \kappa_n\mathcal{C}_n, \quad \mathcal{S} = Se^{\sigma_* S} = \text{diag}(e^{\sigma_*}, -e^{-\sigma_*}). \quad (6.3)$$

So either $\kappa_n = \alpha_*^{3n}$ and \mathcal{C}_n is diagonal (we may assume that the trace is zero), or else $\kappa_n = -e^{\pm 2\sigma_*}\alpha_*^{3n}$ and \mathcal{C}_n has a single nonzero entry, off the diagonal. Many of these eigenvalues are indeed observed numerically, but only for $n > 0$.

6.2. Commutators

Let $P = (F, G)$ with $F = (1, B)$ and $G = (\alpha_*, A)$. We assume that $A = A_* + \mathcal{O}(\varepsilon)$ and $B = B_* + \mathcal{O}(\varepsilon)$ depend smoothly on a parameter ε . Notice that, to first order in ε , the right hand side of (4.1) depends on ε only through the factor Θ^{-1} . Consider now the equation (4.3) that relates the commutator $(0, \tilde{C})$ for the renormalized pair $\tilde{P} = \mathfrak{R}_3(P)$ to the commutator $(0, C)$ for P . Substituting $C_1 = \mathbf{1} + \varepsilon\mathcal{C} + \mathcal{O}(\varepsilon^2)$ and $\tilde{C}_1 = \mathbf{1} + \varepsilon\tilde{\mathcal{C}} + \mathcal{O}(\varepsilon^2)$ into (4.3), and equating terms of order ε , we obtain

$$\tilde{\mathcal{C}}(z) = -A_1(z)^{-1}\mathcal{C}(\alpha_*^3 z)A_1(z). \quad (6.4)$$

Consider now an eigenvector of $\mathcal{C} \mapsto \tilde{\mathcal{C}}$. Near $z = 0$ we have $\mathcal{C}(z) = z^n[\mathcal{C}_n + \mathcal{O}(1)]$ for some nonnegative integer n . Denoting the eigenvalue by η_n , we must have

$$\eta_n\mathcal{C}_n = -\alpha_*^{3n}A_1(0)^{-1}\mathcal{C}_nA_1(0). \quad (6.5)$$

Recall from Proposition 4.1 that $A_1(0)$ has two distinct eigenvalues θ and $\bar{\theta} = \theta^{-1}$ whose squares are non-real. This implies e.g. that there exists a nonzero linear combination of $\mathbf{1}$ and $A_1(0)$ that has a zero trace. This yields a solution \mathcal{C}_n of (6.5) with eigenvalue $\eta_n = -\alpha_*^{3n}$. Many of these eigenvalues are indeed observed in our computations, including $\eta_0 = -1$. The non-real solutions $\eta_n = -\theta^{\pm 2}\alpha_*^{3n}$ are not observed (within the accuracy used). This indicates that non-commuting perturbations contract under renormalization, with the possible exception of one direction with eigenvalue -1 . We note that this applies to \mathfrak{R}_3 but not necessarily \mathfrak{R}^3 .

Remark 1. The equations (6.3) and (6.5) are merely restrictions on eigenvalues that could arise from coordinate transformations and commutators, respectively. To find out more, one needs to determine the associated eigenvectors. If an eigenvector violates a constraint like reversibility, or if it is due to having replaced Λ_3 by Λ_* , then it is not observed in our analysis.

6.3. The second largest eigenvalue

We conclude this section with a formal argument supporting the conjecture that the derivative of \mathfrak{R}^3 at P_* has an eigenvalue α_*^{-3} associated with a change of the strength of the x -dependence. A different argument can be found in [36].

Consider the RG iterates (F_n, G_n) for a commuting pair (F, G) , as described by the equation (5.1). Taking $F = (1, \mathbf{1})$, the matrix part A_n of G_n has the trace

$$\text{tr}(A_n(x)) = \text{tr}(\mathcal{P}_{q_n}(\alpha, \alpha_*^n x)), \quad \mathcal{P}_q(\alpha, x) \stackrel{\text{def}}{=} A(x + (q-1)\alpha) \cdots A(x + \alpha)A(x). \quad (6.6)$$

Here q_n denotes the $n+1^{\text{st}}$ Fibonacci number. Let now G be the AM map with $\lambda \leq 1$, and with $\xi = 0$ for simplicity. Based on our findings described in Section 2, we can expect the trace (6.6) to be arbitrarily close to $\text{tr}(A_*(x))$, if n is chosen sufficiently large and (α, E) sufficiently close to (α_*, E_*) . Then the eigenvalues of $A_n(x)$ have to cover a nontrivial range of values near ± 1 , as x is varied, since the same is true for $A_*(x)$.

In order to determine these eigenvalues approximately, let us use the well-known Chambers formula: if $\gcd(p, q) = 1$, then

$$\text{tr}(\mathcal{P}_q(p/q, x)) = \mathcal{E} - 2\lambda^q \cos(2\pi qx), \quad (6.7)$$

where \mathcal{E} denotes the value of the left hand side for $x = (4q)^{-1}$. Consider $\alpha = p/q$. Choose $q = q_m$ and $p = q_{m-1}$ with $m \gg n$, say $m - n$ constant but large. Then α is the m -th continued fractions approximant for α_* , and $q_m \sim \alpha_*^{-n}$. Presumably, we can choose $E = E_n(\lambda)$ near E_* in such a way that $\mathcal{E} = 3$, and such that $G = (\alpha, A)$ has a zero rotation number for at least one starting point x .

Notice that G has a nonzero rotation number $\text{rot}(G)$ for a given x if and only the trace (6.7) takes values between ± 2 . But, unless λ is sufficiently close to 1, this trace is larger than 2 for all x , in which case G is purely hyperbolic. In order to avoid this, consider taking a limit $\lambda = \lambda_n \rightarrow 1$, in such a way that the right hand side of (6.7) approaches 2 for $x = 0$. (Recall that $\mathcal{E} = 3$.) Then

$$1 - \lambda_n \simeq -\log(\lambda_n) \simeq \frac{\log(4/3)}{q_m} \simeq C\alpha_*^n. \quad (6.8)$$

This accumulation rate suggests that $D\mathfrak{R}^3(P_*)$ has an unstable direction with eigenvalue α_*^{-3} , related to the variation of the parameter λ in the AM model.

7. Computer estimates

What remains to be done is to verify Lemma 3.1 and Proposition 4.1. This is carried out with the aid of a computer. This part of the proof is written in the programming language Ada [39] and can be found in [38]. The following is meant to be a rough guide for the reader who wishes to check the correctness of our programs.

Included in [38] are two files `approx-Fix` and `ContrMat.134`, which contain the approximate fixed point \bar{P} and the (finite rank) operator M , respectively, that enter the definition (3.10) of the transformation \mathfrak{M} .

The main parts of the proof are described in the Ada package `Taylors1.Skews.Pairs`, using procedures defined in several lower-level packages. The main program `Check_Fixpt` first instantiates the required packages with the appropriate parameters, then reads \bar{P} and M from the above-mentioned files, and finally handles control to the procedure `ContrFix`

in `Taylors1.Skews.Pairs`. To give a rough idea of what happens next: `ContrFix` first computes an upper bound ε on the norm of $\mathfrak{M}(0)$, and an upper bound K on the norm of $D\mathfrak{M}(p)$ that holds for all p of norm 4ε or less. After checking that $K < 3/4$, a number $\delta < 4\varepsilon$ is chosen in such a way that $\varepsilon + K\delta < \delta$.

These steps yield accurate and rigorous bounds on all quantities involved. So the last statement in Lemma 3.1, as well as Proposition 4.1, are trivial to verify in this process. In this context, a “bound” on a map $f : \mathcal{X} \rightarrow \mathcal{Y}$ is a function F that assigns to a set $X \subset \mathcal{X}$ of a given type (`Xtype`) a set $Y \subset \mathcal{Y}$ of a given type (`Ytype`), in such a way that $y = f(x)$ belongs to Y for all $x \in X$. In Ada, such a bound F can be implemented by defining an appropriate procedure `F(X: in Xtype; Y: out Ytype)`.

Enclosures for real numbers are defined by data of type `Ball`. For common finite-dimensional spaces we use types `Vector`, `Matrix`, and `Polynom1`. Our type `Taylor1` provides enclosures for functions in the spaces \mathcal{A}_ρ . Basic bounds for this type are defined in the package `Taylors1`. For a detailed description we refer to [32], where the same type has been used. Enclosures for matrix function in \mathcal{A}_ρ^4 are implemented by the type `Skew` defined in the package `Taylors1.Skews`. And for pairs in \mathcal{B}_ρ we use a type `Skew2` defined in `Taylors1.Skews.Pairs`.

Among the procedures defined in `Taylors1.Skews` is a bound `Prod_GFG` on the product $(F, G) \mapsto GFG$ for reversible matrix functions. Notice that the result is again reversible. Combined with a bound `Inv` on $F \mapsto F^{-1}$, `Prod_GFG` is used to compute the composed map $GF^{-1}G$ that appears in the first component of $\mathfrak{R}(P)$. The second component involves $FG^{-1}FG^{-1}F$, which can be computed by applying `Prod_GFG` twice. A bound on the scaling $(F, G) \mapsto (\Lambda_3^{-1}F\Lambda_3, \Lambda_3^{-1}G\Lambda_3)$ is defined by the procedure `Equalize`. The normalization map \mathcal{N} and its derivative (3.8) are bounded via `Normalize` and `DNormalize`, respectively. A bit more complex are the derivative bounds `DProd_GFG` and `DEqualize`. But it should not be difficult to understand the code and verify its correctness.

Bounds on the transformations \mathfrak{R}_3 , \mathfrak{F} , \mathfrak{M} , and their derivatives are obtained simply by composing the bounds described above.

We will not explain here the more basic ideas and techniques underlying computer-assisted proofs in analysis. This has been done to various degrees in several other papers, including [31,32]. As far as our proof of Lemma 3.1 and Proposition 4.1 is concerned, the ultimate reference is the source code of our programs [38]. For the center of the type `Ball` we use high precision [42] floating-point numbers (type `MPFloat`), and for the radii we use standard [41] extended floating-point numbers (type `LLFloat`). Both types support controlled rounding. Our programs were run successfully on a standard desktop machine, using a public version of the `gcc/gnat` compiler [40]. Instructions on how to compile and run these programs can be found in the file `README` that is included with the source code in [38].

Acknowledgments. The author would like to thank Gianni Arioli and Saša Kocić for helpful discussions, and Saša Kocić for drawing my attention to the Hofstadter butterfly.

Data Availability. The source code and data files that represent the technical details of our proofs of Lemma 3.1 and Proposition 4.1 are openly available in `figshare`

at <https://doi.org/10.6084/m9.figshare.11879211> (source code)
 and <https://doi.org/10.6084/m9.figshare.11879205> (data), respectively.

References

- [1] P.G. Harper, *Single band motion of conduction electrons in a uniform magnetic field*, Proc. Phys. Soc. Lond. A **68**, 874–892 (1955).
- [2] D.R. Hofstadter, *Energy levels and wave functions of Bloch electrons in rational and irrational magnetic fields*, Phys. Rev. B **14**, 2239–2249 (1976).
- [3] L.P. Kadanoff, *Scaling for a critical Kolmogorov–Arnold–Moser trajectory*. Phys. Rev. Lett. **47**, 1641–1643 (1981).
- [4] R.S. MacKay, *Renormalisation in Area Preserving Maps*. Thesis, Princeton (1982). World Scientific, London (1993).
- [5] J. Bellissard, B. Simon, *Cantor spectrum for the almost Mathieu equation*, J. Funct. Anal. **48**, 408–419 (1982).
- [6] R. Johnson, J. Moser, *The rotation number for almost periodic potentials*, Commun. Math. Phys. **84**, 403–438 (1982).
- [7] J. Avron, B. Simon, *Almost periodic Schrödinger operators. II. The integrated density of states*, Duke Math. J. **50**, 369–391 (1983).
- [8] S. Ostlund, S. Kim, *Renormalization of quasiperiodic mappings*, Physica Scripta T **9**, 193–198 (1985).
- [9] C. DeConcini, R.A. Johnson, *The algebraic-geometric AKNS potentials*, Ergodic Theory Dynam. Syst. **7**, 1–24 (1987).
- [10] D.J. Thouless, *Scaling for the discrete Mathieu equation*, Commun. Math. Phys. **127**, 187–193 (1990).
- [11] M. Rychlik, *Renormalization of cocycles and linear ODE with almost-periodic coefficients*, Invent. Math. **110**, 173–206 (1992).
- [12] Y. Last, M. Wilkinson, *A sum rule for the dispersion relations of the rational Harper’s equation*, J. Phys. A **25**, 6123–6133 (1992).
- [13] P.B. Wiegmann, A.V. Zabrodin, *Quantum group and magnetic translations. Bethe ansatz solution for the Harper’s equation*, Modern Phys. Lett. B **8**, 311–318 (1994).
- [14] Y. Last, *Zero measure spectrum for the almost Mathieu operator*, Comm. Math. Phys. **164**, 421–432 (1994).
- [15] J. Bellissard, A. van Elst, H. Schulz-Baldes, *The Non-Commutative Geometry of the Quantum Hall Effect*, J. Math. Phys. **35**, 5373–5451 (1994).
- [16] Y. Last, *Almost everything about the almost Mathieu operator. I*, In: XIth International Congress of Mathematical Physics (Paris, 1994), pp. 366–372, Cambridge MA: Internat. Press, 1995.
- [17] J.A. Ketoja, I.I. Satija, *Self-similarity and localization*, Phys. Rev. Lett. **75**, 2762–2765 (1995).
- [18] Y. Hatsugai, M. Kohmoto, Y.-S. Wu, *Quantum group, Bethe ansatz equations, and Bloch wave functions in magnetic fields*, Phys. Rev. B **53**, 9697–9712 (1996).
- [19] A. Stirnemann, *Towards an Existence Proof of MacKay’s Fixed Point*, Comm. Math. Phys. **188**, 723–735 (1997).
- [20] A.Y. Gordon, S. Jitomirskaya, Y. Last, B. Simon, *Duality and singular continuous spectrum in the almost Mathieu equation*, Acta Math. **178**, 169–183 (1997).
- [21] A. Rüdinger, F. Piéchon, *Hofstadter rules and generalized dimensions of the spectrum of Harper’s equation*, J. Phys. A **30**, 117–128 (1997).

- [22] S. Jitomirskaya, *Metal-insulator transition for the almost Mathieu operator*, Ann. of Math. **150**, 1159–1175 (1999).
- [23] B.D. Mestel, A.H. Osbaldestin, B. Winn, *Golden mean renormalisation for the Harper equation: the strong coupling fixed point*, J. Math. Phys. **41**, 8304–8330 (2000).
- [24] D. Osadchy, J.E. Avron, *Hofstadter butterfly as quantum phase diagram*, J. Math. Phys. **42**, 5665–5671 (2001).
- [25] R. Krikorian, *Global density of reducible quasi-periodic cocycles on $\mathbf{T}^1 \times \mathrm{SU}(2)$* , Ann. of Math. (2) **154**, 269–326 (2001).
- [26] B.D. Mestel, A.H. Osbaldestin, *A garden of orchids: a generalized Harper equation at quadratic irrational frequencies*, J. Phys. A **37**, 9071–9086 (2004).
- [27] A. Avila, R. Krikorian, *Reducibility or nonuniform hyperbolicity for quasiperiodic Schrödinger cocycles*, Ann. of Math. **164**, 911–940 (2006).
- [28] D. Damanik, *The spectrum of the almost Mathieu operator*, Lecture series in the CRC 701 (2008).
- [29] M. Goldstein, W. Schlag, *Fine properties of the integrated density of states and a quantitative separation property of the Dirichlet eigenvalues*, Geom. Funct. Anal. **18**, 755–869 (2008).
- [30] A. Avila, D. Damanik, *Absolute continuity of the integrated density of states for the almost Mathieu operator with non-critical coupling*, Invent. Math. **172**, 439–453 (2008).
- [31] G. Arioli, H. Koch, *The critical renormalization fixed point for commuting pairs of area-preserving maps*, Comm. Math. Phys. **295**, 415–429 (2010).
- [32] G. Arioli, H. Koch, *Existence and stability of traveling pulse solutions for the FitzHugh-Nagumo equation*, Nonlinear Analysis A. **113**, 51–70 (2015).
- [33] I.I. Satija, *A tale of two fractals: the Hofstadter butterfly and the integral Apollonian gaskets*, Eur. Phys. J. Spec. Top. **225**, 2533–2547 (2016).
- [34] H. Koch, *On hyperbolicity in the renormalization of near-critical area-preserving maps*, Discrete Contin. Dyn. Syst. **36**, 7029–7056 (2016).
- [35] Sequence [A049651](#) at The On-Line Encyclopedia of Integer Sequences.
- [36] H. Koch, S. Kocić, *Renormalization and universality of the Hofstadter spectrum*, Nonlinearity **33**, 4381–4389 (2020).
- [37] H. Koch, *A symmetric period 6 of the renormalization operator for skew-product maps over circle rotations*, Unpublished.
- [38] H. Koch. The source code for our programs, and data files, are available at figshare with DOI [10.6084/m9.figshare.11879211](#) and DOI [10.6084/m9.figshare.11879205](#), respectively.
- [39] Ada Reference Manual, ISO/IEC 8652:2012(E), available e.g. at www.adc-auth.org/arm.html
- [40] A free-software compiler for the Ada programming language, which is part of the GNU Compiler Collection; see gnu.org/software/gnat/
- [41] The Institute of Electrical and Electronics Engineers, Inc., *IEEE Standard for Binary Floating-Point Arithmetic*, ANSI/IEEE Std 754–2008.
- [42] The MPFR library for multiple-precision floating-point computations with correct rounding; see www.mpfr.org/